J. Ocean Eng. Mar. Energy (2015) 1:145–156
DOI 10.1007/s40722-014-0011-1

RESEARCH ARTICLE

Changing forms and sudden smooth transitions of tsunami waves

R. H. J. Grimshaw · J. C. R. Hunt · K. W. Chow

Received: 14 August 2014 / Accepted: 1 December 2014 / Published online: 13 December 2014
© Springer International Publishing AG 2014

Abstract In some tsunami waves travelling over the ocean, such as the one approaching the eastern coast of Japan in 2011, the sea surface of the ocean is depressed by a small metre-scale displacement over a multi-kilometre horizontal length scale, lying in front of a positive elevation of comparable magnitude and length, which together constitute a down-up wave. Shallow water theory shows that the latter travels faster than the former, leading to an interaction, whose description is the issue addressed in this paper, using model equations of the Korteweg–de Vries type. First, we re-examine the undular bore solutions of the Korteweg–de Vries equation which describe how an initial depression wave deforms into a depression rarefaction wave followed by an undular bore of large elevation waves riding on this depression. Then we develop a new extended Korteweg–de Vries equation some of whose solutions can be used to describe the interaction of an elevation wave chasing a depression wave. These show that the two waves coincide at a given position and time producing a maximum elevation. Typically this amplitude is larger than the initial displacement magnitude by a factor which can be as large as two, which may explain anomalous elevations of tsunamis at particular positions along their trajectories. It is physically significant that for these small amplitude waves, no wave breaking occurs and there is no excess dissipation. Then, following the transition, the elevation wave moves ahead of the depression wave and the distance between them increases either linearly or logarithmically with time. The implications for how these down-up tsunami waves reach the shoreline are considered.

R. H. J. Grimshaw (✉) · J. C. R. Hunt
Department of Mathematics, University College London, London, UK
e-mail: R.H.J.Grimshaw@lboro.ac.uk

K. W. Chow
Department of Mechanical Engineering, University of Hong Kong, Pokfulam, Hong Kong

1 Introduction

Tsunamis are generated by submarine earthquakes, and sometimes by landslides or volcanic eruptions. In general the tsunami wave at the source can be either a wave of depression, or of elevation, or a combination of these, see the recent assessments by Dutykh and Dias (2007), Arcas and Segur (2012) and Dias et al. (2014). As the wave propagates shorewards over the continental slope and shelf, and finally impacting the shoreline, the increasing effect of nonlinearity will lead to quite different set of behaviours depending on the wave polarity, see Carrier et al. (2003) and Fernando et al. (2008) for instance. Although the depression waves can cause as much or more damage than elevation waves, they have not been studied as much as elevation waves. However, their potential importance has been noted in the theoretical studies by Tadepalli and Synolakis (1994, 1996), in the analysis of field data by Soloviev and Mazova (1994) and in the experiments of Kobayashi and Lawrence (2004), Klettner et al. (2012), Rossetto et al. (2011) and Charvet et al. (2013).

Most studies of the connection between the incident wave shape and polarity, and the consequent shoreline impact, have used the linear and nonlinear shallow water equations, see Tadepalli and Synolakis (1994, 1996), Carrier et al. (2003), Madsen and Schaffer (2010) and Didenkulova and Pelinovsky (2011) for instance. In particular, we especially note in the context of this paper the analyses using the nonlinear shallow water equations by Didenkulova (2009), Didenkulova et al. (2006, 2007), and Pelinovsky (2006) which demonstrate the role of initial nonlinear steepness in increasing the eventual runup height, and that by

Didenkulova et al. (2014) who found that this nonlinear steepness effect was enhanced when the initial wave was one of depression. However, although these models have proved valuable and insightful, they are non-dispersive and hence do not capture the effects of wavenumber dispersion as the tsunami waves develop shorter length scales in their propagation shoreward. In particular when shocks are predicted by these models, the discontinuity needs to be resolved either with some turbulent wave-breaking model, or by the inclusion of some wave dispersion. The latter choice is the focus of this paper, where our aim is to exhibit some exact solutions of certain model equations, whose range of dynamical behaviour is potentially interesting in the context of tsunamis when these involve depression waves, and interactions between depression and elevation waves.

The combination of weak nonlinearity and weak linear dispersion leads typically to a Korteweg–de Vries (KdV) equation, or to a Bousinesq system, see Segur (2007) and related articles in the compilation by Kundu (2007) for the tsunami context. However, much of the tsunami literature has focussed on the classical solitary wave solution, which is always a wave of elevation. Hence, in this paper, we use a suite of KdV-type equations to examine how waves of depression evolve. In particular, we will find that this brings out the important role of the undular bore solutions of the KdV models, as found in some tsunami observations and numerical simulations, see Arcas and Segur (2012) and Grue et al. (2008) for instance. It is pertinent to note here that the critique of the validity of KdV models by Madsen et al. (2008), Madsen and Schaffer (2010) and Arcas and Segur (2012), amongst others, are based on solitary wave dynamics, and we suggest that this is a quite restrictive view of the value of KdV theories.

In Sect. 2 we re-examine the KdV equation, Eq. (1) below, both for a constant depth, and for variable depth, with the main aim of demonstrating the structure of depression waves, and the role of the undular bore solutions. Then in Sect. 3 we present an extended KdV equation model, expressed in terms of an augmented dependent variable, which contains both quadratic and cubic nonlinearity, with coefficients of the same positive sign as the linear dispersive term. This model is admittedly *phenomenological* in that while the form of the nonlinear terms can be rigorously justified, the dispersive regularisation with a linear term is admittedly ad hoc and probably cannot be obtained with a systematic asymptotic expansion. This model is formally fully nonlinear, with weak linear dispersion, and in that sense can be regarded as a unidirectional version of the two-way Su-Gardner equations (see El et al. 2006 for a description of these equations). This extended KdV equation contains families of 2-soliton solutions and also breather solutions, which demonstrate striking interactions between depression waves and elevation waves. This interaction typically produces an elevation amplitude which is larger than the initial displacement magnitudes by a factor which can be as large as two. We conclude in Sect. 4.

We are especially concerned with the scenario when the approaching tsunami wave, propagating with a speed c which depends on the depth h, and also on the wave amplitude, consists of a depression wave of magnitude $\Delta h \ll h$ and horizontal length scale $L_0 \gg h$, in front of an elevation wave of comparable magnitude, constituting a down-up wave, or isosceles N-wave in the terminology of Tadepalli and Synolakis (1994). This configuration was observed in the Sumatra tsunami of 2004, see Ioulalen et al. (2007) and Grilli et al. (2007), and that in Tohoku in 2011 see Mori et al. (2013), and was examined in experiments by Klettner et al. (2012) motivated in part by these observations. Such a structure depends of course on the shape of the co-seismic bottom displacements, see the theoretical analysis by Dutykh and Dias (2007) for instance. Shallow water theory implies that the elevation will travel faster with a speed difference $\Delta c \sim \sqrt{g\Delta h}$, and then after a time $t^* \sim L_0/\Delta c$ the waves undergo a transition. First, the two parts coincide and produce a maximum elevation $\beta\Delta h$, where based on the afore-mentioned 2-soliton and breather solutions, we estimate that $1 \le \beta \le 2$ and $\beta = 2$ when the depression and elevation waves are of equal amplitude magnitudes. Second, the elevation wave then moves ahead of the depression wave and the distance between them increases in proportion to $(t - t^*)$ or $\log(t - t^*)$ for the 2-soliton or breather solutions, respectively. These estimates may explain anomalous elevations of some tsunamis at particular positions along their trajectories, noting that for these small amplitude waves, there is very little dissipation.

2 Korteweg–de Vries equation

The Korteweg–de Vries equation on a variable depth is

$$\zeta_t + c\zeta_x + \frac{c_x}{2}\zeta + \frac{3c}{2h}\zeta\zeta_x + \frac{ch^2}{6}\zeta_{xxx} = 0. \tag{1}$$

Here $\zeta(x,t)$ is the free surface elevation above the undisturbed depth $h(x)$, while $c(x) = \sqrt{h(x)}$ is the linear long wave phase speed, using non-dimensional units based on a length scale h_0 and a time scale $\sqrt{h_0/g}$. Equation (1) was derived for surface gravity waves by Johnson (1973a, b) and an analogous general equation for both surface and internal waves by Grimshaw (1981). The first two terms in (1) are the dominant terms and by themselves describe the propagation of a linear long wave with speed c. The derivation uses the usual KdV balance in which the $\partial/\partial x \sim \epsilon \ll 1$, $A \sim \epsilon^2$, and weak inhomogeneity is added so that c_x/c scales as ϵ^3.

Equation (1) is in the form appropriate for an initial value problem. For application to tsunami waves, it is useful to cast it into a form describing evolution along the wave path. Thus,

a form asymptotically equivalent to (1) is

$$\zeta_\tau + \frac{h_\tau}{4h}\zeta + \frac{3}{2h}\zeta\zeta_\xi + \frac{h}{6}\zeta_{\xi\xi\xi} = 0, \tag{2}$$

$$\text{where} \quad \tau = \int_0^x \frac{\mathrm{d}x'}{c(x')}, \qquad \xi = \tau - t. \tag{3}$$

Here τ is a time-like variable measuring travel time along the wave path, and in variable depth, $h = h(\tau)$. This governing Eq. (2) can be cast into several equivalent forms.

$$\eta = h^{1/4}\zeta \quad \text{so that} \quad \eta_\tau + \frac{3}{2h^{5/4}}\eta\eta_\xi + \frac{h}{6}\eta_{\xi\xi\xi} = 0. \tag{4}$$

This form shows that Eq. (2) has two integrals of motion with the densities proportional to $\eta = h^{1/4}\zeta$ and $\eta^2 = h^{1/2}\zeta^2$. These are often referred to as laws for the conservation of "mass" and "momentum" (more correctly, wave action flux). Another useful form is

$$U = \frac{3\eta}{2}, \quad U_\sigma + 6UU_\xi + h^{9/4}U_{\xi\xi\xi} = 0, \tag{5}$$

$$\sigma = \frac{1}{6}\int_0^\tau \frac{\mathrm{d}\tau'}{h^{5/4}(\tau')} = \frac{1}{6}\int_0^x \frac{\mathrm{d}x'}{h^{7/4}(x')}. \tag{6}$$

In this formulation we assume that $h = 1$ when the depth is constant and then $h < 1$ when the wave moves up a slope.

On a constant depth the KdV equation (5) has the well-known soliton (solitary wave) solution

$$U = A\,\mathrm{sech}^2(K(\xi - V\sigma)), \quad V = 2A = 4K^2. \tag{7}$$

Here we are concerned with the "initial" value problem when $U = U_0(\xi)$ at $\sigma = 0$. Note that this is in fact a specification of a wave at an initial location, and the equation then describes the spatial evolution. It is well known that if $U_0(\xi) \geq 0$ (elevation), then several solitons are generated, but if instead $U_0(\xi) \leq 0$, (depression) then no solitons are generated, and instead the solution disperses with the front being described by a nonlinear Airy-type function. This has the shape of an initial depression, followed by a series of elevation waves riding on a negative pedestal, see El (2007), Segur (2007) and Arcas and Segur (2012) for instance.

Consider, for example, the case when $U_0(\xi) = \pm G(\xi)$, respectively, an initial wave of elevation, or depression, where $G(\xi) \geq 0$ is a localised pulse, for instance a Gaussian. Then in the elevation case, N rank-ordered solitons are produced, with N amplitudes, together with some trailing dispersing radiation. When N is large, the soliton amplitudes are distributed according to the law

$$A \sim \frac{\xi}{2\sigma}, \quad 0 < \frac{\xi}{4\sigma} < G_M = 2\max G(x). \tag{8}$$

In particular the leading emerging solitary wave has an amplitude of $2G_M$, see El (2007).

In the depression case the long-time evolution can be modelled as a rarefaction wave [an exact solution of (5)] given by

$$\begin{aligned} &U = 0, \quad \xi > 0, \\ &U = \frac{\xi}{6\sigma}, \quad -L(\sigma) < \frac{\xi}{6\sigma} < 0, \\ &U = 0, \quad \frac{\xi}{6\sigma} < -L(\sigma), \\ &\text{where} \quad 3\sigma L^2 = M = \int_{-\infty}^{\infty} |G(\xi)|\,\mathrm{d}\xi. \end{aligned} \tag{9}$$

Here $L(\sigma)$ is determined by conservation of mass. This solution is an N-wave, and at $\xi = 6\sigma L$, there is jump L from the negative level $-L$ to 0. This is resolved by an undular bore whose leading wave is a solitary wave of amplitude $2L$, relative to the pedestal of $-L$, see Grimshaw (2001) and El (2007) for instance. Thus the amplitude of this leading solitary wave is $2(M/3\sigma)^{1/2}$. This can be larger than the leading solitary wave from an elevation initial condition, when $\sigma < M/3G_M^2$. Note that here M, G_M are independent parameters, and this estimate suggests that the leading elevation wave on a depression wave emanating from a depression initial condition will be greater than the leading elevation wave from an elevation initial condition when M is large, but G_M is small. The laboratory experiments of Hammack and Segur (1978) exhibit this behaviour, see their Figs. 2 and 3, also reproduced in the review by Arcas and Segur (2012).

When there is a slope, there are no analogous asymptotic solutions available. However it is known that a single solitary wave will deform adiabatically as h^{-1}, see El et al. (2012) and the references therein. However, the numerical study by El et al. (2012) indicates that a KdV undular bore of elevation propagating up a slope develops a quite complicated structure, but the leading solitary wave does deform as h^{-1}. When the initial wave is one of depression, then the rarefaction wave of depression (9) again holds even when h in Eq. (5) varies. Hence we would again expect an undular bore to develop at the trailing edge, with the leading solitary wave in the undular bore deforming adiabatically. Indeed, this behaviour was found in the experiments by Klettner et al. (2012) describing of an initial depression up a slope, see their Fig. 5 especially.

3 Extended Korteweg–de Vries equation

3.1 Derivation

The extended Korteweg–de Vries equation (eKdV) for water waves on a constant depth is an extension of (1) when a cubic

nonlinear term is included:

$$\zeta_t + c\zeta_x + \frac{3c}{2h}\zeta\zeta_x + \alpha\zeta^2\zeta_x + \frac{ch^2}{6}\zeta_{xxx} = 0. \tag{10}$$

The coefficient α can be found from the literature, see Marchant and Smyth (1990) for instance, or more directly by noting that in the absence of dispersion, the Riemann invariant solution from nonlinear shallow water theory is

$$R_t + VR_x = 0, \quad R = U + 2C, \quad V = U + C,$$
$$C = \sqrt{h+\zeta}, \quad L = U - 2C = -2\sqrt{h}. \tag{11}$$

Here R, L are the right-going and left-going Riemann invariants, and the left-going wave has been set to the constant background. Hence,

$$\zeta_t + V\zeta_x = 0, \quad V = 3\sqrt{h+\zeta} - 2\sqrt{h}$$
$$= c + \frac{3c}{2h}\zeta - \frac{3c}{8h^2}\zeta^2 + \cdots. \tag{12}$$

Hence we infer that $\alpha = -3c/8h^2$, which is the opposite sign to that needed for the eKdV equation to have breather solutions.

However, noting that the coefficient α is not unique, here we adopt a different approach. First we note that (11) can be expressed in terms of V:

$$V_t + VV_x = 0. \tag{13}$$

Indeed, this is exact and shows that in terms of the variable V, $\alpha = 0$. More generally the Riemann invariant equation (12) can be written as

$$Z_t + VZ_x = 0 \quad Z = Z(\zeta), \quad V = V(Z), \tag{14}$$

where $Z(\zeta)$ can be chosen arbitrarily. We choose Z so that

$$V(Z) = c + \frac{3c}{2h}Z + \frac{3c\beta}{2h^2}Z^2. \tag{15}$$

Here $\beta > 0$ can be chosen arbitrarily. Then combining this with the expression for $V(\zeta)$ in (12) defines the function $Z(\zeta)$:

$$\left(1 + \frac{\zeta}{h}\right)^{1/2} - 1 = \frac{Z}{2h} + \frac{\beta Z^2}{2h^2},$$
$$\text{so that} \quad Z(\zeta) = \zeta - \left(\frac{1}{4} + \beta\right)\frac{\zeta^2}{h} + \cdots. \tag{16}$$

Thus in the limit when $\zeta \ll h$, we infer that (16) is a near-identity transformation as then $Z \approx \zeta$.

The nonlinear hyperbolic equation (14) with $V(Z)$ given by (15) is a valid right-going solution of the nonlinear shallow water equations. Next we consider its dispersive regularisation and here we make the ad hoc assumption that a linear dispersive term will suffice, noting that this is certainly valid in the small-amplitude limit. Thus we obtain the following eKdV equation for the augmented variable Z:

$$Z_t + cZ_x + \frac{3c}{2h}ZZ_x + \frac{3c\beta}{2h^2}Z^2Z_x + \frac{ch^2}{6}Z_{xxx} = 0. \tag{17}$$

Since the dispersive term has been approximated by a linear term, but we have kept the fully nonlinear relationship between Z and ζ in (16), this is a *phenomenological* model. In this sense it can be regarded as a unidirectional version of the two-way Su-Gardner equations (see El et al. 2006 for a description of these equations). Nevertheless, we suggest that its solutions may be relevant, at least in part, to the study of down-up tsunami waves. Importantly in this application, we can choose $\beta > 0$ and so this model eKdV equation has a positive coefficient of the cubic nonlinear term. Next we put (17) into canonical form:

$$Z = \frac{hv}{\beta}, \quad x - ct = \hat{\beta}hX, \; t = \frac{6\hat{\beta}^3 hT}{c}, \quad \hat{\beta} = \left\{\frac{2\beta}{3}\right\}^{1/2}, \tag{18}$$

$$v_T + 6vv_X + 6v^2v_X + v_{XXX} = 0. \tag{19}$$

The transformation (16) then becomes

$$\left(1 + \frac{\zeta}{h}\right)^{1/2} - 1 = \frac{1}{2\beta}(v + v^2). \tag{20}$$

Note that $-1 < \zeta/h < 0$ only when $-1 < v < 0$, and the minimum value of the left-hand side is -1, while the minimum value of the right-hand side is $-1/4\beta$ when $v = -1/2$. Hence we must choose $\beta \geq 1/4$, but otherwise β is a free parameter. The choice $\beta = 1/4$ allows a full range of negative values of ζ, but otherwise the range of ζ/h is bounded below by $\zeta_{\min}/h = -1/2\beta + 1/16\beta^2$. Importantly, note that solutions for which $v < -1$ are such that $\zeta/h > 0$. It is useful to note that choosing $\beta \gg 1$ implies that $\zeta/h \ll 1$, assuming that v is order unity, and then the left-hand side of (20) can be approximated by $\zeta/2h$.

3.2 Solitons and breathers

The eKdV equation (19) is integrable and has an associated inverse scattering transform and families of soliton and breather solutions, see Grimshaw et al. (2010) for instance. The soliton and breather solutions can be found using a variety of methods, including the Darboux transformation, see Slunyaev (2001), and the Hirota bilinear method, see Chow et al. (2005). The latter yields

$$v = 2\left\{\tan^{-1}\left(\frac{g}{f}\right)\right\}_X = \frac{2}{f^2 + g^2}(fg_X - gf_X), \tag{21}$$

where f, g are expressed in terms of exponential functions, sometimes including algebraic terms.

3.2.1 1-soliton solution

The 1-soliton solution is given by

$$g = 1 + sa\exp(\gamma Y), \quad f = 1 + sb\exp(\gamma Y),$$
$$Y = X - \gamma^2 T, \quad a, b = \frac{1 \pm \gamma}{\sqrt{1+\gamma^2}}, \quad s = \pm 1,$$
$$v = \frac{\gamma^2}{1 + s\sqrt{1+\gamma^2}\cos h(\gamma Y)}. \tag{22}$$

Here $s = \pm 1$ corresponds to an elevation wave of amplitude $A = \sqrt{\gamma^2+1} - 1$ and a depression wave of amplitude $A = -\sqrt{\gamma^2+1} - 1$, respectively. As γ varies over the range $0 < \gamma < \infty$ the elevation wave amplitude lies in the range $0 < A < \infty$, while the depression wave amplitude lies in the range $-2 > A > -\infty$. For the same speed, the depression wave has the larger amplitude magnitude, but for the same amplitude magnitude, the elevation wave is faster. In general, the elevation wave with index 1 is faster than the depression wave with index 2 when $\gamma_1 > \gamma_2$, but will have the smaller amplitude magnitude when $\sqrt{1+\gamma_1^2} - 1 < \sqrt{1+\gamma_2^2} + 1$, which is always the case when $\gamma_1^2 < 8$, and remains the case unless γ_1^2 is sufficiently large, and sufficiently greater than γ_2^2.

Importantly, the terms depression and elevation relate to the augmented variable v and not to the original variable ζ. Although the 1-soliton solution (22) does generate a 1-soliton solution for ζ through the transformation (20), both the depression and elevation waves for v have positive amplitudes for ζ. This is as it should be, since for water waves (in the absence of strong surface tension) we do not expect to find *steady* solitary waves of depression. Both the elevation soliton and the depression soliton for v generate steady solitary waves for ζ with the same speed γ^2 in the X, T variables, but with different profiles and amplitudes. The elevation soliton ($s = 1$ in (22)) generates a solitary wave of elevation for ζ with a monotonic profile on each side of the crest, which in the limit of small amplitudes $\gamma \to 0$ reduces to the expected KdV solitary wave. On the other hand, the depression soliton ($s = -1$ in (22)) generates a solitary wave with two negative side-lobes, corresponding to the domain $0 > v > -1$, and then a central elevation corresponding to the domain $-1 > v > -1 - \sqrt{1+\gamma^2}$ whose amplitude is greater than the amplitude of the elevation soliton. Although such a steady solitary wave is not expected to exist in the full water wave problem, it is nonetheless interesting in the present context as indicating that a depression wave followed by an elevation wave can have a larger central amplitude than the corresponding elevation wave.

3.2.2 2-soliton solutions

Now consider a 2-soliton solution with far-field parameters γ_1, γ_2, given by, adapted from (11) in Chow et al. (2005):

$$g = 1 + s_1 a_1 \exp(\phi) + s_2 a_2 \exp(\psi) + s_1 s_2 a_{12} \exp(\phi + \psi),$$
$$f = 1 + s_1 b_1 \exp(\phi) + s_2 b_2 \exp(\psi) + s_1 s_2 b_{12} \exp(\phi + \psi),$$
$$\phi = \gamma_1 X - \gamma_1^3 T, \quad \psi = \gamma_2 X - \gamma_2^3 T,$$
$$a_n, b_n = \frac{1 \pm \gamma_n}{\sqrt{1+\gamma_n^2}}, \quad n = 1, 2,$$
$$a_{12}, b_{12} = \frac{(\gamma_1 - \gamma_2)^2}{(\gamma_1 + \gamma_2)^2} \frac{[1 \pm (\gamma_1 + \gamma_2) - \gamma_1\gamma_2]}{\sqrt{1+\gamma_1^2}\sqrt{1+\gamma_2^2}}. \tag{23}$$

Without loss of generality, take $\gamma_2 > \gamma_1$. In the far field as $T \to \pm\infty$ the soliton limits are found by either fixing the phase ϕ and letting $\psi \to \mp\infty$ for the index 1, or fixing the phase ψ and letting $\phi \to \pm\infty$ for the index 2. The outcome is, for index 1,

$$g \sim 1 + s_1 a_1 \exp(\phi), \quad f \sim 1 + s_1 b_1 \exp(\phi), \quad T \to \infty,$$
$$g \sim a_2 + s_1 a_{12} \exp(\phi), \; f \sim b_2 + s_1 b_{12} \exp(\phi), \; T \to -\infty, \tag{24}$$

and for index 2,

$$g \sim a_1 + s_2 a_{12} \exp(\psi), \; f \sim b_1 + s_2 b_{12} \exp(\psi), \quad T \to \infty,$$
$$g \sim 1 + s_2 a_2 \exp(\psi), \; f \sim 1 + s_2 b_2 \exp(\psi), \quad T \to -\infty. \tag{25}$$

Note that common factors in f, g can be removed. Each of these are easily recognised as the corresponding 1-soliton solutions, but with a phase shift from $T \to -\infty$ to $T \to \infty$, given by

$$\exp(-\Delta\phi), \exp(\Delta\psi) = \frac{(\gamma_2 + \gamma_1)^2}{(\gamma_2 - \gamma_1)^2}. \tag{26}$$

This agrees with the expression (11) in Slunyaev (2001). Note that $\Delta\phi < 0$, $\Delta\psi > 0$, so the faster wave is shifted forwards and the slower wave is shifted backwards.

Our interest here is in the case when the depression wave precedes the elevation wave as $T \to -\infty$, so that the depression and elevation wave have indices 1, 2, respectively, that is $s_1 = -1$, $s_2 = 1$. Then the elevation wave will catch up with the depression wave, and there will be an interaction at the approximate location $X = 0$, $T = 0$. Taking account of the phase shifts (26) this can be refined to $X = X_{\text{int}}$, $T = T_{\text{int}}$ where

$$(\gamma_2^2 - \gamma_1^2) X_{\text{int}} = -\frac{\gamma_1^2 \Delta\phi}{2\gamma_1} - \frac{\gamma_1^2 \Delta\psi}{2\gamma_2},$$
$$(\gamma_2^2 - \gamma_1^2) T_{\text{int}} = -\frac{\Delta\phi}{2\gamma_1} - \frac{\Delta\psi}{2\gamma_2}. \tag{27}$$

Further, we can deduce from the preceding expressions that if the two waves are located a distance $2X_0$ apart at a time $\pm T_0$ as $T \to \pm\infty$, then

$$2X_0 \approx (\gamma_2^2 - \gamma_1^2)T_0. \tag{28}$$

Note that both expressions (27, 28) will fail when $\gamma_2 \to \gamma_1$. Slunyaev (2001) (see Eq. (10)) provides an estimate that at the interaction centre the amplitude is $A_2 - A_1$, where $A_1 < 0$, $A_2 > 0$ are the far-field amplitudes. The interaction is like that of a breather, and at the centre there is enhanced elevation, lying between $2\min[A_1, A_2]$ and $2\max[A_1, A_2]$. This is twice the far-field value when $|A_1| = A_2$. A set of typical results are shown in Figs. 1 and 2 for the cases when $\gamma_1 = 0.7, \gamma_2 = 3.0$ and $\gamma_1 = 1.3, \gamma_2 = 3.4$, respectively. These represent two solitons of nearly equal amplitudes, $A_1 = -2.22, A_2 = 2.16$ and $A_1 = -2.64, A_2 = 2.54$, respectively, so that the depression wave is slightly larger in magnitude, but considerably slower in speed. Then in Figs. 3 and 4 we plot the cases when $\gamma_1 = 0.7, \gamma_2 = 0.72$ and $\gamma_1 = 1.3, \gamma_2 = 1.5$ so that now the speeds are quite close, but the elevation wave is faster, while the amplitudes are quite different with a much larger depression wave, $A_1 = -2.22, A_2 = 0.23$ and $A_1 = -2.64, A_2 = 0.8$, respectively. These cases are similar to Figs. 3 and 4 of Slunyaev (2001), but there the speeds were much faster.

As for the 1-soliton solution, each expression (23) for a 2-soliton solution for the variable v generates a corresponding 2-soliton-like structure for ζ through the transformation (20). Although in the far field these solutions separate into two distinct solitary waves for ζ as described in Sect. 3.2.1, our main interest here is in the interaction shown in the central panels of Figs. 1, 2, 3 and 4. Significantly in each of these v varies from a minimum negative value of around -1 to a maximum positive value ranging from 2 to 5. Then the negative values of v will correspond to negative values of ζ and the positive values of v to positive values of ζ so that the qualitatively the structure shown will be similar for ζ.

3.2.3 Breather solutions

The breather solution can be found by formally putting $\gamma_{1,2} = m \pm in$, $m, n > 0$ in (23), see (14) in Slunyaev (2001), or (13) in Chow et al. (2005). The outcome is, obtained here by setting $s_1 = s_2 = 1$ and adjusting the phases appropriately,

$$g = 1 - \frac{n^2}{m^2}\frac{1 + 2m - (m^2 + n^2)}{1 - 2m + (m^2 + n^2)}\exp(2m\theta) + 2(\xi\cos(n\Theta) - \eta\sin(n\Theta))\exp(m\theta),$$

$$f = 1 - \frac{n^2}{m^2}\frac{1 - 2m - (m^2 + n^2)}{1 - 2m + (m^2 + n^2)}\exp(2m\theta) + 2\cos(n\Theta)\exp(m\theta),$$

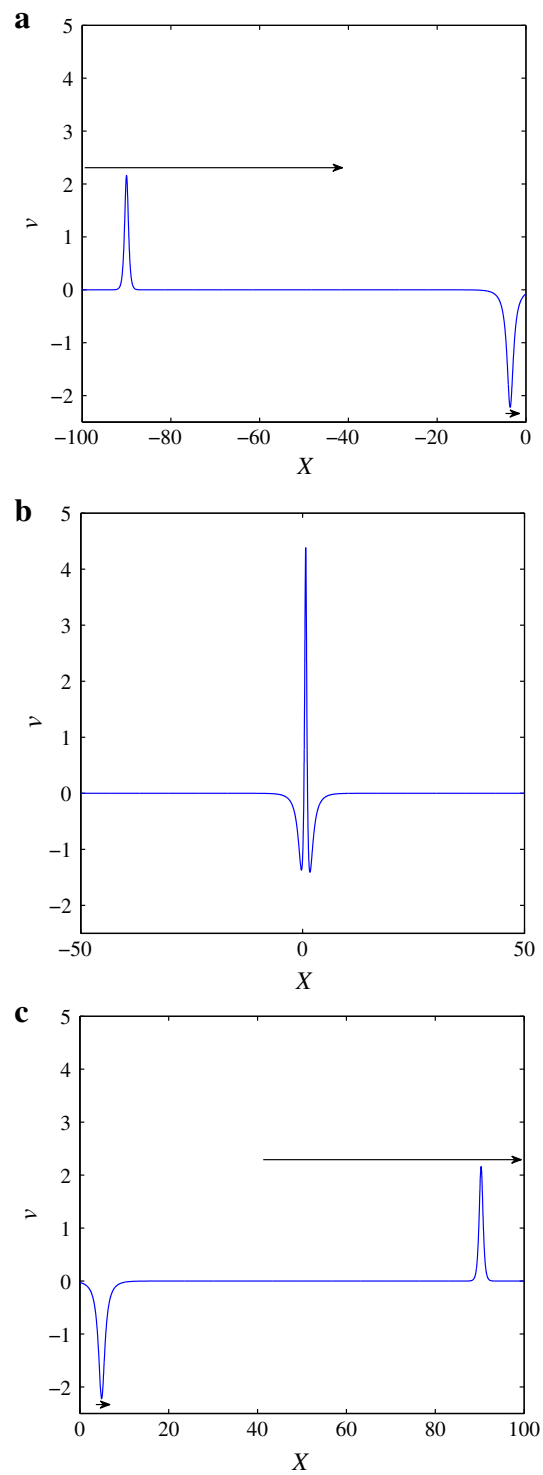

Fig. 1 Plot of (23) for $\gamma_1 = 0.7, \gamma_2 = 3.0$ at $t = -10, 0.06, 10$ from *top* to *bottom*. The arrows in **a** and **c** indicate the direction of the waves, and their lengths are proportional to the respective speeds, $\gamma_{1,2}^2$

$$\theta = X - (m^2 - 3n^2)T, \quad \Theta = X - (3m^2 - n^2)T,$$

$$\xi = \frac{1 - (m^2 + n^2)}{1 - 2m + m^2 + n^2}, \quad \eta = \frac{2n}{1 - 2m + m^2 + n^2}. \tag{29}$$

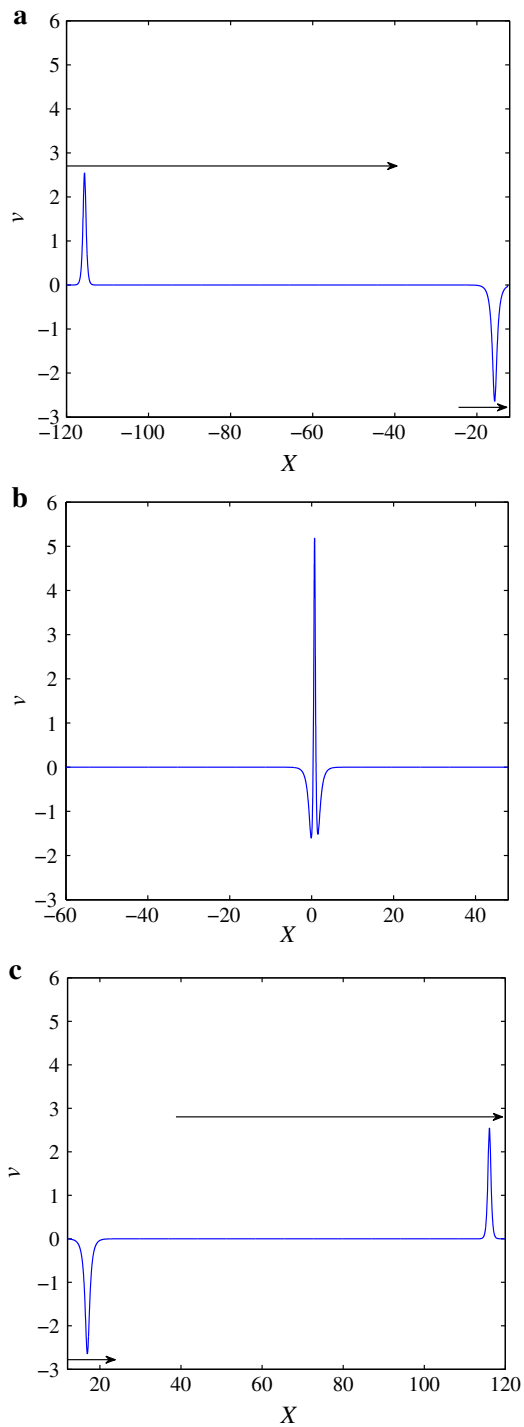

Fig. 2 Plot of (23) for $\gamma_1 = 1.3$, $\gamma_2 = 3.4$ at $t = -10, 0.04, 10$ from *top* to *bottom*. The arrows have the same meaning as in Fig. 1

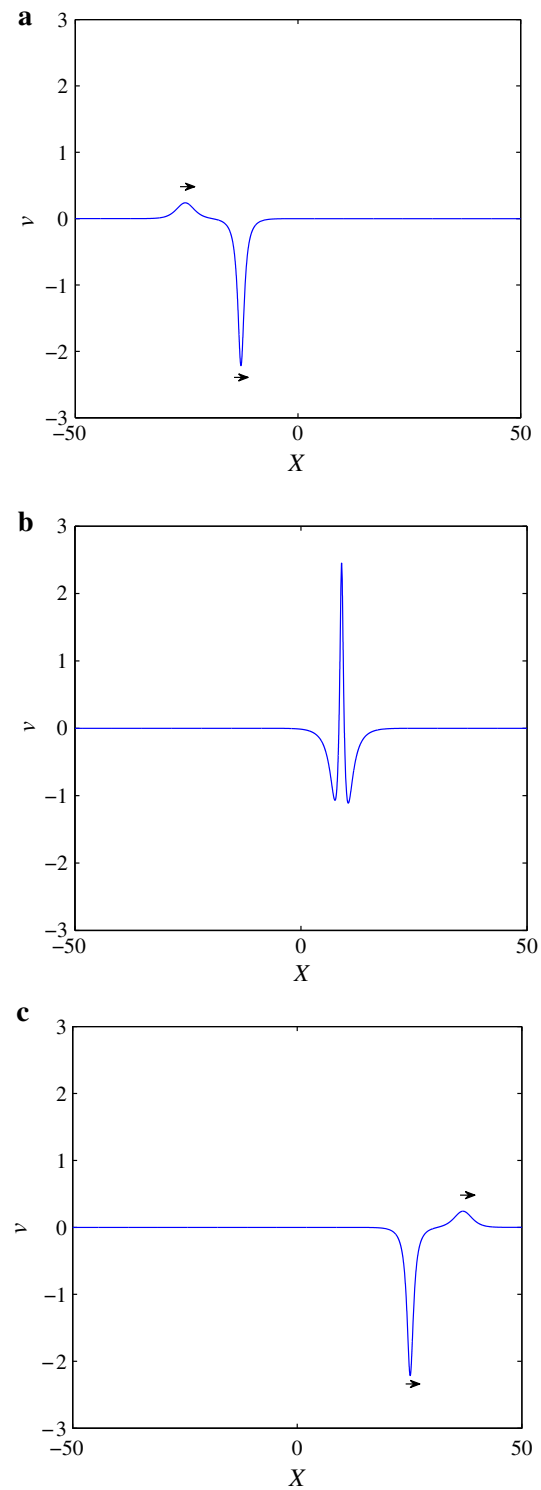

Fig. 3 Plot of (23) for $\gamma_1 = 0.7$, $\gamma_2 = 0.72$ at $t = -50, 5.95, 50$ from *top* to *bottom*. The arrows have the same meaning as in Fig. 1

The breather has two phases, θ and Θ. It is localised in the phase θ and propagates with a speed $C = m^2 - 3n^2$, and oscillates in the phase Θ with a frequency $n\Omega$, $\Omega = 3m^2 - n^2$. In the reference frame moving with speed C, set $Y = X - CT$ and then $\Theta = n(Y - 2(m^2 + n^2))T$. Hence in this frame it has a period

$$P = \pi / n(m^2 + n^2). \tag{30}$$

In the limit $n \gg m$ there are many crests inside the envelope and it resembles an envelope wave packet. In the opposite limit when $n \ll m$, it resembles a 2-soliton interaction, see

Fig. 5 of Slunyaev (2001) or Fig. 4 of Chow et al. (2005). This is the case of interest here and describes the interaction of two solitons of opposite polarity and almost equal speeds. Hence the depression soliton has the larger amplitude. The greatest distance apart is

$$L = \frac{2}{m} \log \frac{2m}{n}. \tag{31}$$

The double pole solution can be found by again choosing special phases and taking the limit $n \to 0$ in (29), see Chow et al. (2005):

$$\begin{aligned} g &= 1 - \frac{1 + 2m - m^2}{m^2(1-m)^2} \exp(2m\theta) \\ &\quad + \frac{2[(1-m^2)\Theta + 2] \exp(m\theta)}{(1-m)^2}, \\ f &= 1 - \frac{1 - 2m - m^2}{m^2(1-m)^2} \exp(2m\theta) + 2\Theta \exp(m\theta), \\ \theta &= X - m^2 T, \quad \Theta = X - 3m^2 T = \theta - 2m^2 T. \end{aligned} \tag{32}$$

A typical result is shown in Fig. 4 of Chow et al. (2005). In the far field as $T \to -\infty$ this is an elevation wave chasing a larger amplitude depression wave. They coincide around $T = 0$, and then as $T \to \infty$ the elevation wave goes ahead. In detail, for fixed phase θ, as $T \to \pm\infty$, the solution collapses to two single waves, each approximately a single wave, propagating with speed $V \sim m^2$, and hence with expected amplitudes $\sim \pm\sqrt{1+m^2} - 1$, see (22). Each wave phase can be described asymptotically for large $|T|$ by

$$m\theta \sim \pm \mathrm{sign}\{T\} \log(Km^2|T|), \text{ so that } \quad V \sim m^2 \pm \frac{1}{m|T|}, \tag{33}$$

where the alternate signs refer to the faster/slower wave, respectively. K is a positive constant to be determined and depends both on which wave is being considered, and on which limit, that is either $T \to \pm\infty$. The speeds become equal in the long time limit, and the two waves separate as $\log|T|$. From (32), we can write $v = 2N/D$, $D = f^2 + g^2 > 0$, and

$$\begin{aligned} N &= f g_X - g f_X = \Theta[\alpha_3 \exp(3m\theta) + \alpha_1 \exp(m\theta)] \\ &\quad + [\beta_3 \exp(3m\theta) + \beta_2 \exp(2m\theta) + \beta_1 \exp(m\theta)], \\ \alpha_3 &= -\frac{4(1+m^2)}{(1-m)^3}, \quad \alpha_1 = \frac{4m^2}{(1-m)}. \end{aligned} \tag{34}$$

Note that $\alpha_3 < 0, \alpha_1 > 0$ when $0 < m < 1$, and $\alpha_3 > 0, \alpha_1 < 0$ when $m > 1$. These expressions can be evaluated on the trajectories (33), where we note that then $\Theta \sim -m^2 T$ with a logarithmic error. As $T \to -\infty$, $\exp(m\theta) \sim (Km^2|T|)^{\mp 1}$, and as $T \to \infty$, $\exp(m\theta) \sim (Km^2|T|)^{\pm 1}$, for the faster and slower waves, respectively.

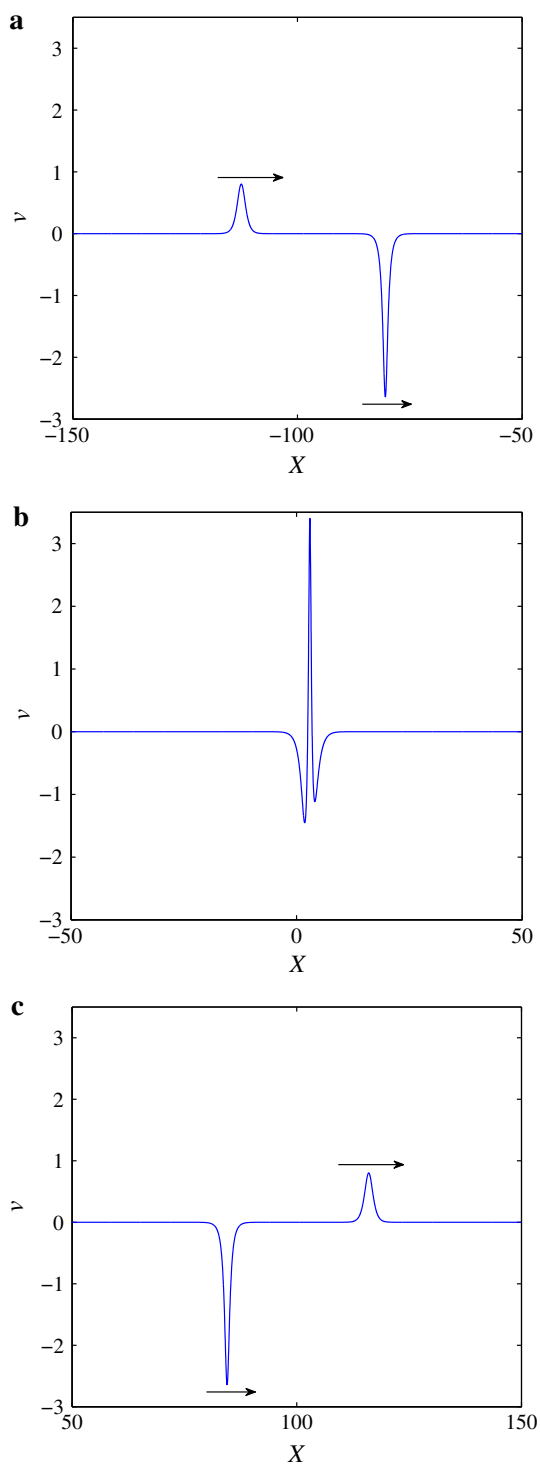

Fig. 4 Plot of (23) for $\gamma_1 = 1.3, \gamma_2 = 1.5$ at $t = -50, 0.5, 50$ from *top* to *bottom*. The arrows have the same meaning as in Fig. 1

It then follows that, for the faster wave,

$$N \sim \frac{\alpha_1}{K},\ \ D \sim (1+\frac{2}{K})^2 + (1+\frac{2a_1}{K})^2,\ \ T \to -\infty,$$
$$N \sim -m^8K^3\alpha_3T^4,\ D \sim m^8K^2T^4$$
$$\{(f_1K+2)^2 + (g_1K+2\alpha_1)^2\},\ T \to \infty. \tag{35}$$

Here f_1, g_1 are the coefficients of the term $\exp(2m\theta)$ in the expressions (32) for f, g, respectively. In both limits, the amplitude is a constant as required, and is positive for $0 < m < 1$ and negative for $m > 1$. For the slower wave,

$$N \sim m^8K^3\alpha_3T^4,\ D \sim m^8K^2T^4$$
$$\{(f_1K-2)^2 + (g_1K-2\alpha_1)^2\},\ \ T \to \infty.$$
$$N \sim -\frac{\alpha_1}{K},\ \ D \sim (1-\frac{2}{K})^2 + (1-\frac{2a_1}{K})^2,\ \ T \to -\infty, \tag{36}$$

Again, in both limits, the amplitude is a constant as required, and is now negative for $0 < m < 1$ and positive for $m > 1$. Note that only the leading order term in N is needed here in all cases, and the term in $[\cdots]$ is not needed. Also we see that $|2N/D|$ depends on K and in all cases is zero as $K \to 0, \infty$ and has a maximum value when

$$K = \frac{2(1+m^2)^{1/2}}{|1-m|},\ \text{Cases } f_-, s_+;$$
$$K = \frac{2m^2|1-m|}{(1+m^2)^{1/2}},\ \text{Cases } f_+, s_-. \tag{37}$$

Here the notation $f_\pm, s_\pm$ denotes the faster or slower wave as $T \to \pm\infty$, respectively. Then evaluation of the corresponding amplitudes $2N/D$ at these values of K are indeed $\pm\sqrt{1+m^2} - 1$ according as the wave is one of elevation or depression, as expected. Using these expressions we can deduce from (33) that the faster and slower wave have phase shifts from $T \to \infty$ to $T \to \infty$ of $\pm\Delta\theta$ where

$$\Delta\theta = \log\{\frac{1+m^2}{m^2(1-m)^2}\}. \tag{38}$$

Finally, we can deduce from the phase expressions (33) that if the two waves are located a distance $2X_0$ apart at a time $\pm T_0$ as $T \to \pm\infty$, then

$$mX_0 \approx \log(2m^3T_0). \tag{39}$$

Plots of (32) for $m = 0.7, 1.3$ are shown in Figs. 5 and 6, respectively. Note that Fig. 5 is similar to Fig. 4 of Chow et al. (2005), and also to the 2-soliton solution shown in Figs. 3 and 4 above, although note that as discussed above, the time scale of approach and separation are quite different for this breather case. The amplitudes at $t = \pm 50$ are in good agreement with the theoretical predictions as $t \to \pm\infty$ indicating that the asymptotic state has been reached. In Fig. 5 where $0 < m < 1$ the faster wave is one of elevation and the slower wave is one of depression. At the time of interaction, which is close to $T = 0$ and can be estimated from the phase shifts (38), we see that these waves combine into a large elevation whose height is approximately given by the

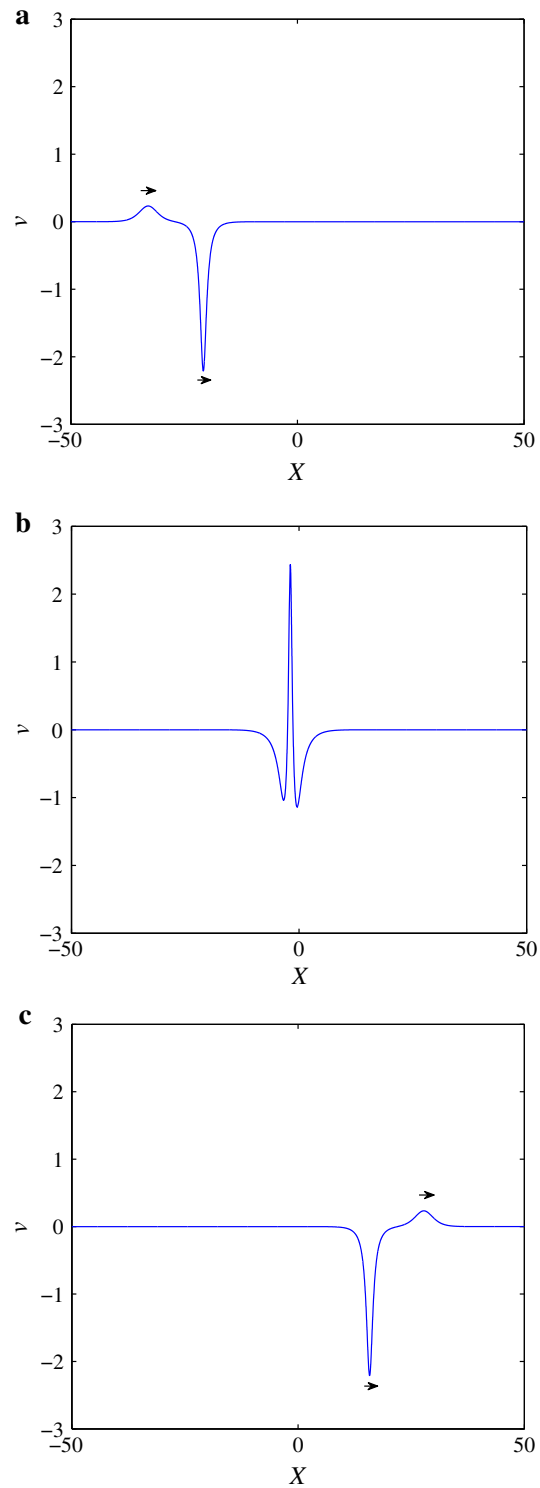

Fig. 5 Plot of (32) for $m = 0.7$ at $t = -50, 1.3, 50$ from *top* to *bottom*. The arrows have the same meaning as in Fig. 1

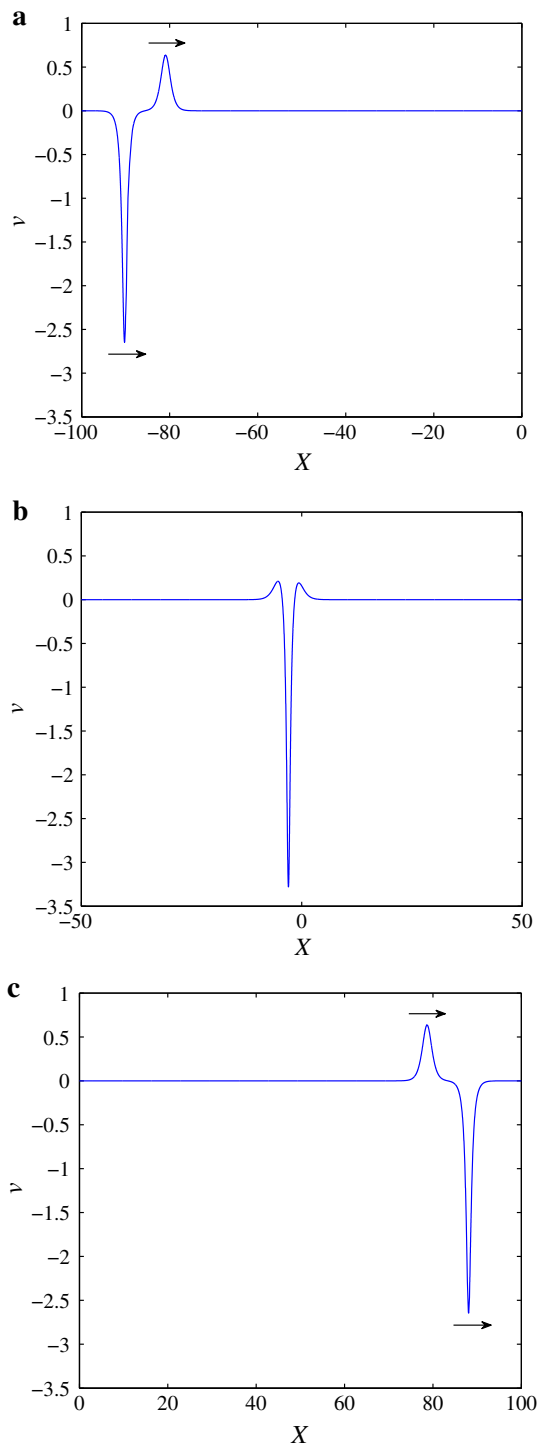

Fig. 6 Plot of (32) for $m = 1.3$ at $t = -50, -1.15, 50$ from *top* to *bottom*. The arrows have the same meaning as in Fig. 1

absolute sum of the amplitudes at infinity, which is given here by $2\sqrt{1+m^2}$. This scenario is reversed in Fig. 6 where $m > 1$ as now the faster wave is one of depression and the slower wave is one of elevation, with the consequence that at the time of interaction the waves combine into a large depression whose amplitude is approximately $-2\sqrt{1+m^2}$.

Again, as for the 2-soliton solution, the expression (32) for a breather solution for the variable v generates a corresponding breather-like structure for ζ through the transformation (20). Our main interest here is in the interaction shown in the central panels of Fig. 5 where significantly v varies from a minimum negative value of around -1 to a maximum positive value ranging from 2. Then the negative values of v will correspond to negative values of ζ and the positive values of v to positive values of ζ so that the qualitatively the structure shown will be similar for ζ. However, this in not the case for the middle panel of Fig. 6 where the large negative peak for v will generate a more complicated structure for ζ.

4 Discussion and applications

In this paper we have used the traditional KdV model (Sect. 2) and a new eKdV model (Sect. 3) to examine the dynamics of a down-up wave, that is a depression wave followed by an elevation wave. This approach differs from the extensive literature on N-waves found using the usual non-dispersive nonlinear shallow water equations, in that these models importantly include the effects of weak linear wave dispersion. We note that Arcas and Segur (2012) recently called attention to the necessity to invoke wave dispersion when describing tsunami waves of depression. The KdV model, whether for a constant depth, or on a slope, indicates that an initial depression develops into a depression wave followed by a series of elevation waves riding on this negative pedestal, see Arcas and Segur (2012) for instance, and the leading wave may have an amplitude magnitude twice that of the leading depression. We have already noted that this scenario is qualitatively similar to that seen in the wave tank experiments of Klettner et al. (2012) where an initial wave of depression travelled up a slope. When the expressions in Eq. (9) and the following text are translated to the original dimensional variables through the transformations in Eqs. (3)–(6), we find that the predicted height of the leading solitary wave is $2L_d$, $L_d = 2(4M_d h/3x_d)^{1/2}$, riding relative to a pedestal of $-L_d$ where M_d is the initial total displaced volume, and x_d is the distance travelled. From Fig. 5a of Klettner et al. (2012) we estimate that $M_d = 0.03\,\mathrm{m}^2$ and then when $x_d = 20.68\,\mathrm{m}$ we find that $L_d = 0.04\,\mathrm{m}$, in quite good agreement with the observed value of about 0.05 m. Note that here we have not taken account of the wave amplification over the slope,and this would account for the underestimate. Indeed at the location x_d the depth in the wave tank has decreased from 0.8 to 0.7 m and assuming the adiabatic expression of h^{-1} for a solitary wave, this would increase our estimate of L_d to $L_d = 0.046\,\mathrm{m}$.

However, in these KdV models this combination of a depression and elevation waves is an unsteady wave train, and so the complete structure eventually fully disperses. Hence in a search for models supporting more persistent structures, we have invoked a higher-order model, the eKdV equation (17), or in scaled form (19). Although this eKdV model supports interacting depression and elevation waves through families of 2-soliton and breather solutions, we must note that as already discussed, this is a *phenomenological* model and its application to water waves requires caution. Specifically, there are two issues concerning the application of this model. First, we note again that the balance of terms in (17) is such that the nonlinear terms have a larger magnitude than the linear dispersive term. If a small-amplitude hypothesis is invoked to remedy this, then the outcome is that the cubic nonlinear term is suppressed *vis-a-vis* the quadratic nonlinear term. This then eliminates the depression soliton, the 2-soliton solution, when comprising both elevation and depression waves, and the breather solution of interest here, as all these require a balance between the quadratic and cubic nonlinear terms. Second, although one might accept that (17) and (19) can be used in the ad hoc sense that the role of the linear dispersive term is to provide a weak dispersive regularisation of the fully nonlinear equation (14) which is valid within the fully nonlinear shallow water framework, the application to water waves requires use of the relationship $v(\zeta)$ expressed in (20), and then again $Z \approx \zeta$ only when $\zeta \ll h$. Nevertheless, we maintain that portions of these solutions have qualitative features which resemble laboratory and field observations of some tsunami waves and suggest that this eKdV model does have value when properly interpreted. In particular we focus on the interaction scenarios displayed in the middle panel of Figs. 1, 2, 3, 4 and 5 as here the solutions are predominately positive and as discussed above the relationship $v(\zeta)$ in (20) leads to a qualitatively similar scenario and hence to useful physical interpretation.

The expressions presented in Sect. 3.2 provide a complete explicit description of the interaction of depression and elevation waves (in the v-variable), and from these we can extract the essential information on the timescale for the interaction, and the wave amplitude at the centre of the interaction (expressed in terms of the ζ-variable on using the transformation (20). There are two main kinds of 2-soliton interaction: one in which the depression and elevation components have similar amplitudes, shown in Figs. 1, 2 and the other in which the two components have similar speeds, shown in Figs. 3, 4. The double-pole breather solution, shown in Figs. 5, 6, is essentially a limit of the 2-soliton interaction when the speeds are identical. From the analytical expressions we can estimate a dimensional transition time, taking account of the scaling (18) and using the transformation (20) in the small-amplitude limit. Thus suppose that initially an elevation wave of amplitude Δh_2 is located at $x = -L_0$ behind a depression wave of amplitude $-\Delta h_1$ located at $x = +L_0$. The speed of each wave can be estimated from (12) as $c(1 \pm \Delta h_{1,2}/2h)$. From the 2-soliton model these two approach each other linearly in time, see (28), and interact at a time and place given by

$$t^* \approx \frac{4hL_0}{c\zeta_{\text{int}}}, \quad x^* \approx \frac{4hL_0}{\zeta_{\text{int}}}, \quad \text{where} \quad \zeta_{\text{int}} = \Delta h_2 + \Delta h_1. \tag{40}$$

Here we also assumed that $\Delta h_{1,2} \ll h$, and ζ_{int} is the estimated elevation at the interaction site. On the other hand, from the double-pole breather model, the approach is logarithmic in time and the corresponding expressions for t^*, x^* can be deduced from (39). However, then the interaction time and place are increased exponentially due to the slower logarithmic approach, and we find that these alternative expressions are not as applicable as (40). For instance, based on the available data recorded near Phuket Island for the Sumatra 2004 tsunami, see Ioulalen et al. (2007) and Grilli et al. (2007), we choose $\Delta h_2 = 3\,\text{m}$, $\Delta h_1 = 3\,\text{m}$, $h = 25\,\text{m}$, $L_0 = 8\,\text{km}$, and then $t^* = 142\,\text{min}$, $x^* = 133\,\text{km}$ and $\zeta_{\text{int}} = 6\,\text{m}$. These estimates indicate that the peak interaction is close to the shoreline, although the bottom slope has not been taken into account, which would slow the wave interaction down and so reduce x^*. A similar scenario can be deduced from tide gauge data north of Sendai for the Tohoku 2011 tsunami, see Fujii et al. (2011), Shimozono et al. (2012) and Klettner et al. (2012). Here we choose $\Delta h_2 = 4\,\text{m}$, $\Delta h_1 = 4\,\text{m}$, $h = 50\,\text{m}$, $L_0 = 16\,\text{km}$ as representative values, and then $t^* = 301\,\text{min}$, $x^* = 200\,\text{km}$ and $\zeta_{\text{int}} = 8\,\text{m}$. In this case these estimates indicate that the tsunami would reach the shore before the peak interaction occurs.

In conclusion, we suggest that the scenarios we have described here, both for the KdV and the eKdV models, are useful for understanding and possibly predicting the behaviour of down-up tsunami waves. In particular, as the plots we have shown demonstrate, there is a potential that the nonlinear interaction between the depression and elevation components can produce a striking elevation at the location of the interaction. It is to be emphasised that this outcome is more devastating than that caused by an incident elevation wave alone of the same initial height. Although here we have focussed on the 2-soliton and breather solutions of the eKdV equation (19) we note that it was shown by Grimshaw et al. (2010) using a combination of the inverse scattering transform and numerical simulations, that initial conditions consisting either solely of a depression, or a combination of a depression with an elevation, will generically generate solitons of opposite polarity and breathers. Finally, although here we essentially used only qualitative information obtained from the eKdV model to describe tsunami depression waves, it would be interesting to test this model further, for instance

by comparison with numerical simulations of the full equations and also by extension of the model to variable topography. Also we remind that the KdV and eKdV models are developed for non-dissipative flows without any wave breaking and as such conserve momentum flux asymptotically.

Acknowledgments Hester H.N. Chan of the University of Hong Kong, and Kenyon K. Chow of the University of California at Los Angeles, assisted in the preparation of the figures. RHJG and JCRH acknowledge the hospitality of the Mechanical Engineering Department at the University of Hong Kong during their respective visits.

References

Arcas D, Segur H (2012) Seismically generated tsunamis. Phil. Trans. R. Soc. 370:1505–1542

Carrier GF, Wu TT, Yeh H (2003) Tsunami run-up and drawdown on a plane beach. J. Fluid Mech. 475:79–99

Charvet I, Eames I, Rossetto T (2013) New tsunami run-up relationships based on long wave experiments. Ocean Modell. 69:79–92

Chow KW, Grimshaw R, Ding E (2005) Interactions of breathers and solitons in the extended Kortewegde Vries equation. Wave Motion 43:158–166

Dias F, Dutykh D, OBrien L, Renzi E, Stefanakis T (2014) On the modelling of tsunami generation and tsunami inundation. Procedia IUTAM 10:338–355

Didenkulova I (2009) New trends in the analytical theory of long sea wave runup. In: Quak E, Soomere T (eds) Applied wave mathematics: selected topics in solids, fluids, and mathematical methods. Springer, Berlin, pp 265–296

Didenkulova II, Zahibo N, Kurkin AA, Levin BV, Pelinovsky EN, Soomere T (2006) Runup of nonlinearly deformed waves on a coast. Doklady Earth Sci 411:1241–1243

Didenkulova I, Pelinovsky E, Soomere T, Zahibo N (2007) Runup of nonlinear asymmetric waves on a plane beach. In: Kundu A (ed) Tsunami and nonlinear waves. Springer, Berlin, pp 175–190

Didenkulova I, Efim Pelinovsky E (2011) Nonlinear wave evolution and run-up in an inclined channel of a parabolic cross-section. Phys. Fluids 23:086602

Didenkulova II, Pelinovsky EN, Didenkulov OI (2014) Run-up of long solitary waves of different polarities on a plane beach. Izvestya Atmos Ocean Phys 50:532–538

Dutykh D, Dias F (2007) Water waves generated by a moving bottom. In: Kundu A (ed) Tsunamis and nonlinear waves. Springer, Berlin, pp. 65–96

El GA, Grimshaw RHJ, Smyth NF (2006) Unsteady undular bores in fully nonlinear shallow-water theory. Phys Fluids 18:027104

El G (2007) Kortweg-de Vries equation and undular bores. In: Grimshaw R (ed) Solitary waves in fluids. Advances in fluid mechanics, vol 47. WIT Press, UK, pp 19–53

El GA, Grimshaw RHJ, Tiong WK (2012) Transformation of a shoaling undular bore. J. Fluid Mech. 709:371–395

Fernando HJS, Braun A, Galappatti R, Ruwanpura J, Wirisinghe SC (2008) Tsunamis: manifestation and aftermath. In: Large scale disasters. Cambridge University Press, Cambridge, pp 258–292

Fujii Y, Sakai S, Shinohara M, Kanazawa T (2011) Tsunami source of the 2011 off the Pacific coast of Tohoku earthquake. Earth Planets Space 63:815–820

Grilli ST, Ioualalen M, Asavanant J, Shi F, Kirby JT, Watts P (2007) Source constraints and model simulation of the December 26, 2004, Indian Ocean tsunami. J Waterway Port Coast Ocean Eng 133:414–428

Grimshaw R (1981) Evolution equations for long nonlinear internal waves in stratified shear flows. Stud Appl Math 65:159–188

Grimshaw R (2001) Internal solitary waves. In: Grimshaw R (ed) Environmental stratified flows. Kluwer, The Netherlands, pp 1–27

Grimshaw R, Slunyaev A, Pelinovsky E (2010) Generation of solitons and breathers in the extended Kortewegde Vries equation with positive cubic nonlinearity. Chaos 20:013102

Grue J, Pelinovsky E, Fructus D, Talipova T, Kharif C (2008) Formation of undular bores and solitary waves in the Strait of Malacca caused by the 26 December 2004 Indian Ocean tsunami. J Geophys Res 113:C05008

Hammack JL, Segur H (1978) The Kortewegde Vries equation and water waves. III. Oscillatory waves. J. Fluid Mech. 84:337–358

Ioualalen M, Asavanant J, Kaewbanjak N, Grilli ST, Kirby JT, Watts P (2004) Modeling, the 26, (December 2004) Indian Ocean tsunami: case study of impact in Thailand. J Geophys Res 112:C07024

Johnson RS (1973a) On an asymptotic solution of the Korteweg–de Vries equation with slowly varying coefficients. J Fluid Mech 60:813824

Johnson RS (1973b) On the development of a solitary wave moving over an uneven bottom. Proc Camb Phil Soc 73:183203

Klettner C, Balasubramanian S, Hunt J, Fernando H, Voropayaev S, Eames I (2012) Draw-down and run-up of tsunami waves on sloping beaches. Eng Comput Mech 165:119–129

Kobayashi N, Lawrence AR (2004) Cross- shore sediment transport under breaking solitary waves. J Geophys Res 109:C03047

Kundu A (2007) In: Kundu A (ed) Tsunamis and nonlinear waves. Springer, Berlin

Madsen PA, Fuhrman DR, Schäffer, HA (2008) On the solitary wave paradigm for tsunamis. J. Geophys. Res. 113:C12012

Madsen PA, Schaffer HA (2010) Analytical solutions for tsunami run-up on a plane beach: single waves, N-waves and transient waves. J Fluid Mech 645:27–57

Marchant TR, Smyth NF (1990) The extended Korteweg–de Vries equation and the resonant flow of a fluid over topography. J Fluid Mech 221:263–288

Mori N, Takahashi T, Yasuda T, Yanagisawa H (2013) Survey of 2011 Tohoku earthquake tsunami inundation and run-up. Geophys Res Lett 38:L00G14

Pelinovsky E (2006) Hydrodynamics of tsunami waves. Chapter 1, waves in geophysical fluids. In: Grue J, Trulsen K (eds) CISM courses and lectures, vol 489. Springer, Berlin, pp 1–48

Rossetto T, Allsop W, Charvet I, Robinson DI (2011) Physical modelling of tsunami using a new pneumatic wave generator. Coast Eng 58:517–527

Segur H (2007) Waves in shallow water, with emphasis on the tsunami of 2004. In: Kundu A (ed) Tsunamis and nonlinear waves. Springer, Berlin, pp 3–29

Shimozono T, Sato T, Okayasu A, Tajima Y, Fritz HM, Liu H, Takagawa T (2012) Propogation and inundation characteristics of the 2011 Tohoku tsunami on the central Sanriku coast. Coast Eng J 54:125004

Soloviev SL, Mazova RK (1994) On the influence of sign of leading tsunami wave on run-up height on the coast. Sci Tsunami Haz 12:2531

Slunyaev AV (2001) Dynamics of localized waves with large amplitude in a weakly dispersive medium with a quadratic and positive cubic nonlinearity. J Exp Theor Phys 92:529–534

Tadepalli S, Synolakis CE (1994) The run-up of N-waves on sloping beaches. Proc R Soc A 445:99–112

Tadepalli S, Synolakis CE (1996) Model for the leading wave of tsunamis. Phys Rev Lett 77:2141–2144